iJRASET
International Journal For Research in Applied Science and Engineering Technology

INTERNATIONAL JOURNAL FOR RESEARCH

IN APPLIED SCIENCE & ENGINEERING TECHNOLOGY

Volume: 14 **Issue:** VIII **Month of publication:** August 2026

DOI: https://doi.org/10.22214/ijraset.2026.84748

www.ijraset.com

Call: 08813907089 | E-mail ID: ijraset@gmail.com

International Journal for Research in Applied Science & Engineering Technology (IJRASET)
ISSN: 2321-9653; IC Value: 45.98; SJ Impact Factor: 7.538
Volume 14 Issue VIII Aug 2026- Available at www.ijraset.com

Investigation of Structural, Electrical and Gamma-Ray Attenuation Characteristics of MnO-Doped Bi_2O_3-H_3BO_3-P_2O_5 Glasses

Mallo Devi[1], Sunil Kumar Dwivedi[2], Pawan Heera[3]
[1]*Scholar, Physics, Om Sterling Global University, Hisar (Haryana)*
[2]*Dept. of Physics, Om Sterling Global University, Hisar (Hryana)*
[3]*Dept. of Physics, Central University of Himachal Pradesh, Himachal Pradesh, Dharamshala, India*

Abstract: ***The importance of development of lead-free glasses for high-performance radiation shielding materials with tailored capacitive characteristics are critical for advanced optoelectronic and radiation protection applications.This study investigates influence of compositional impact of substituent (MnO) asglass network modifier on its structural rearrangements, dielectric performance, and ray attenuation capability.Phosphate Glasses of heavy-metal oxide with stoichiometric proportion of 40 Bi_2O_3–35 H_3BO_3–(25−x) P_2O_5–xMnO, where x = 0.5, 1.0, 1.5, 2.0 and 2.5 mol%, have been prepared using melt-quenching technique. Influence of substitution of MnO as a compositional modifier on capacitive and γ radiation shielding has been reported. Apart from structural investigation such network arrangement, density, molar volume also be studied. In radiation shielding, various parameters such as mass attenuation coefficient (MAC), linear attenuation coefficient (LAC), half-value layer (HVL), tenth-value layer (TVL) &mean free path (MFP) have been calculated to explore influence of MnO as compositional modifier on radiation shielding ability. To get exact information about radiation response of substitution of compositional modifier (MnO) on phosphate glasses (40 Bi_2O_3–35 H_3BO_3–(25−x) P_2O_5–xMnO, where x = 0.5, 1.0, 1.5, 2.0 & 2.5 mol%,), experimentally calculated radiation parameters have been compared with theoretically calculated radiation parameters using measured using a ^{137}Cs source (4.5 μCi, 662 keV), closely aligned with theoretical predictions from XCOM NIST software &source coupled with a Geiger-Müller counter. For electric characteristics, frequency dependent ε'& ε''and σ_{ac} at room temperature be investigate and understand polarization and charge-transport mechanisms. Presence of multivalent manganese ions facilitates small polaron hopping ($Mn^{2+} \leftrightarrow Mn^{3+}$), significantly modulating the dielectric permittivity (ε'& ε''), dielectric loss (Tan□), and AC conductivity as functions of frequency and temperature. Theseobtained results may provide useful information of developing multifunctional phosphate-borate glasses for radiation shielding and radiation-resistant electronic applications.***

Key words: MAC, Gamma Ray Shielding, Glass, Bismuth- Borate.

I. INTRODUCTION

The increasing utilization of ionizing radiation in medical diagnostics, radiotherapy, nuclear power generation, industrial radiography, non-destructive testing and space technology has created a continuing requirement for efficient radiation-shielding materials. Gamma radiation possesses high penetration power and can interact with matter through different mechanisms depending on photon energy and the atomic composition of the absorber. Consequently, the development of dense, stable and compositionally tunable shielding materials remains an important area of materials research. Conventional shielding materials such as lead and concrete are extensively used because of their high attenuation capability. The risks of ionizing radiation coming from natural background, nuclear facilities, and space exploration with associated health risks like cancer and tissue damage are compiled. The study evaluates the feasibility of the radiation shielding materials with respect to their attenuation efficiency, mechanical strength, cost, and ease of production. Radiation-shielding materials should be environmentally friendly, durable, transparent, and easy to produce[1].Concrete is the most commonly used shield material in nuclear reactors because it is inexpensive and adapt-able for any construction design. Although, concrete is widely used for shielding but degrades with time and is thus not suitable for some applications [3]. Glass might be an excellent alternative to concrete as a gamma ray shielding material [2].They can be used in X-rayrooms, for instance, to allow workers to view inside the room where the patient. Glasses doped with heavy metal oxides are promising alternatives because of their high density, effective radiation shielding, and ease of production through melt quenching.B_2O_3 is one of the most commonly used glass formers.

©IJRASET: All Rights are Reserved

However, lead-based materials are associated with toxicity and environmental concerns, whereas concrete-based shields can be bulky, opaque and difficult to shape into compact components. Heavy-metal oxide glasses have therefore attracted considerable attention because they combine relatively high density, compositional flexibility, optical transparency, chemical stability and ease of fabrication. The uploaded reference manuscript similarly emphasizes the importance of heavy-metal oxide glasses as alternatives to conventional shielding materials.Phosphate and borate glasses are particularly attractive because of their good glass-forming ability and relatively low processing temperatures. P_2O_5 is an important glass former capable of producing phosphate structural units, whereas borate species contribute to the connectivity and stability of the glass network. The structural role of phosphate and borate components can be modified significantly by the incorporation of transition-metal oxides. Among heavy-metal oxides, Bi_2O_3 is particularly interesting because bismuth possesses a high atomic number and Bi-containing glasses can exhibit substantial photon attenuation. Bi_2O_3can also participate in modification of the glass network and influence density, optical properties and dielectric behavior. The source manuscript identifies Bi_2O_3 as an important heavy-metal constituent for gamma-ray shielding. B_2O_3 is one of the most commonly used glass formers.It forms moisture resistant and low rate of crystallization glasses with high valent oxides like Bi_2O_3. Borate-based glasses have low viscosity, great mechanical strength, chemical resistance, and transparency, which makes them cost-effective and versatile for biomedical, industrial, and radiation shielding applications [3]. Bismuth-based glasses are noted for their high density and effective gamma-ray shielding qualities when compared to other traditional materials such as certain types of concrete and commercial glass. Glasses containing 20 mol% to 50 mol% bismuth oxide (Bi_2O_3) showed better attenuation coefficients as a superior radiation absorber [5].Role of Bi2O3 has been identified as conditional glass former. It acts as a glass modifier at low concentrations and on the other hand ,it acts as glass former at higher concentration(Maeder*, 2013)(Kaur et al., 2016).Along with other heavy metal oxideslead is particularly valuable due to its availability and its efficiency as a barrier against radiation. Further, lead oxide (PbO) incorporation in glass compositions improves gamma-ray shielding due to its high atomic number and density, effectively attenuating radiation.Research published in Scientific Reports found that adding 10% or 20% lead oxide increased the shielding capabilities of the examined geopolymer, particularly at lower photon energy [1-10]

MnO is an interesting transition-metal oxide for modifying phosphate-borate glasses. Manganese can exist in different oxidation states, principally Mn^{2+} and Mn^{3+}, and therefore can influence the local structural environment and charge-compensation processes within the glass network. The incorporation of MnO may generate changes in non-bridging oxygen concentration, bond distribution, ionic polarizability and localized charge-carrier concentration. Consequently, Mn_2O_3 substitution can influence both dielectric relaxation and electrical conductivity. Small amounts of TeO_2 and P_2O_5 are added to the glass to improve its structural stability and radiation shielding capabilities without compromising process ability. If there are too many of them, the glass will become more brittle (due to TeO_2) and viscous (due to P_2O_5), which will make it more difficult to produce. For producing a good shielding glass, it should have a large interaction cross-section while having minimal impacts from irradiation on its mechanical and optical characteristics [8].

In the present work, Mn_2O_3 is progressively incorporated in matrix $Bi_2O_3 – H_3BO_3$at the expense of P_2O_5 in stoichiometric proportion accordingly:

$$40Bi_2O_3–35H_3BO_3–(25–x)P_2O_5–_xMnO \quad (1)$$

where x=0.5, 1.0, 1.5, 2.0 and 2.5 mol%.

A. Experimental Approach: Synthesis and Characterization

Phosphate Glasses of heavy-metal oxide with stoichiometric proportion of 40 Bi_2O_3–35 H_3BO_3–(25–x) P_2O_5–xMnO, where x = 0.5, 1.0, 1.5, 2.0 and 2.5 mol%, have been prepared using melt-quenching technique. Required metal ion P_2O_5, H_3BO_3, Bi_2O_3 and PbO as mentioned in stoichiometric proportion of AR grade purchased from Sigma Aldrich India are used to prepare Phosphate Glasses of heavy-metal oxide. First for 20 g batch of each composition, all required metal ion weighed in mentioned stoichiometric proportionis mixed well using motar pestle and after complete homogeneous mixing, powder transferred in Alumina crucible and heated at 950^0 C for 3 hours continuously until molten state of until homogeneous mixture is obtained. After melting of powder, crucible taken out and poured in graphite mold and annealed at 400^0C in pre-heated for 30 min followed by slow cooling to room temperature in order to remove internal stress [1-2]. The final product in glass for in cylindrical shape have been obtained and grinded for of different measurement parameters. Chemical composition of the prepared glass samples is provided in Table 1

Sample code	Composition (mole fraction)				Density
	Bi_2O_3	H_3BO_3	MnO	P_2O_5	
S1	0.4	0.35	0.225	0.025	4.50
S2	0.4	0.35	0.23	0.02	4.55
S3	0.4	0.35	0.235	0.015	4.60
S4	0.4	0.35	0.24	0.01	4.58
S5	0.4	0.35	0.245	0.005	4.69

Table 1: Composition, density and molar volume of the glass system

B. Densities and Molar Volumes

Density of prepared Phosphate Glasses of heavy-metal oxide with stoichiometric proportion of 40 Bi_2O_3–35 H_3BO_3–(25−x) P_2O_5–xMnO, where x = 0.5, 1.0, 1.5, 2.0 and 2.5 mol% have been measured by using lab made instrument based on Archimedes' principle and densities are calculated by using formula given below[11, 21]. During this experiment, Glass samples first weighed in air and then immersed in water and weighed and using formula;

$$\text{Density } (\rho) = \frac{W_1}{(W_1 - W_2)} \times \rho_{water} \qquad \textbf{(2)}$$

where W_1 = Sample weight in air

W_2 = Sample weight in water

The molar volume of prepared Phosphate Glasses of heavy-metal oxide with stoichiometric proportion of 40 Bi_2O_3–35 H_3BO_3–(25−x) P_2O_5–xMnO, where x = 0.5, 1.0, 1.5, 2.0 and 2.5 mol% have been calculated by using formulae given below;

$$\textbf{Vm} = \frac{M}{\rho} \qquad \textbf{(3)}$$

where M sample's molar mass of Phosphate Glasses of heavy-metal oxideand ρ is density of Phosphate Glasses of heavy-metal oxidedetermined by using Archimedes' principle.

C. Experimental Determination of Radiation Shielding Properties

The radiation shielding capability of Phosphate Glasses of heavy-metal oxide has been determined by performing shielding experiment carried out with GM counter in presence Cs-137 radioactive isotope which act as radioactive source, gas detector and ST-360 SN329 software interfaced which give helps us to calculate intensity counts of gamma ray shielding. Cylindrical glass samples with diameter 1.5 cm and varying thickness values in the range of 8.1-8.9 mm have been used for γ-ray attenuation measurements. During this experiment, samples first placed one by one between source and the detector as shown in Figure 1. The incident (Io) and transmitted (I) intensities (Table 2) were determined interfaced in GM counter for a fixed preset time (200s). Three observations of each glass sample have been measured by using ST-360 SN329 software. This is a gas based detector which uses ionization of gas by radiations the primary tool to detect radiation. A metallic string which runs through the central axis of the cylindrical shape forms the anode whereas the outer shell serves as cathode. One end of the tube has radiation permeable window (micaorberyllium).

II. THEORY/CALCULATIONS

A. Gamma Ray shielding Properties

The experimental mass attenuation coefficient values were calculated using NaI (TI) detector to detect gamma rays. A ″3.8cm(diameter)×2.5(thick)″ NaI (TI) detector has been used(Peterson, 1996)[pdf]. The detector has an energy resolution of 12.5% at 662 keV. ^{137}Cs has been the source of γ-rays. Approximately 1 mrem of whole-body dosage may be obtained from a 10 μCi, ^{137}Cs encapsulated source that is carried around for 12 hours. An average chest x-ray yields an absorbed dosage of 40–200 mrem(Peterson, 1996). This dosage is normal as we easily work in this environment without serious damage. Each pulse is converted to a channel number using an integrated analog-to-digital converter, allowing each channel to correspond to a small range of pulse heights or voltages(Kaur et al., 2016).

The spectrum is generated by the MCA by arranging the pulse distributions according to height over time(Kaur et al., 2016). This spectrum is viewable on a PC, whose measurement is taken as the mass attenuation coefficient. The thickness values of my obtained samples are ranging from 6.25 to 6.45 mm have been employed to test γ-ray attenuation Shown in Table 2.Each sample was individually positioned between the source and the detector for the measurement of intensity of incoming and outgoing gamma rays. The attenuation coefficient is the process of decreasing photons in a gamma-ray beam when it interacts with materials. Primary photons can be attenuated by absorption, scattering, or pair creation. Attenuation at low energies, below 26 keV, is primarily driven by the photoelectric effect. When high-energy photons interact with low-Z materials, Compton scattering is the primary attenuation process. At photon energies over 1.02 MeV, pair formation has a substantial impact in attenuation. Here we study only about ^{137}Cs as gamma ray source which have photo-peak around 662keV.

The experimental mass attenuation coefficient values for our six compositions are obtained by famous Lambert-Beer law as shown below

$$\mu/\rho = \ln(I_o/I)\,/\rho t\,, \qquad (4)$$

where ρ is the density of the given material, I_o and I are intensity of incoming and outgoing gamma rays and t is the thickness of the material used as absorber. The obtained experimental mass attenuation coefficient values are shown in Table 2.

The term HVL refers to the thickness of the material that reduces gamma radiation by half (50%). Generally, this is directly related to the mass attenuation coefficient shown in Table 2 and is commonly used as a measure to assess shielding effectiveness and is obtained by

$$\text{HVL} = \frac{ln2}{\mu}\,. \qquad (5)$$

where μ is the linear attenuation coefficient.

Mean free path (λ) is the average distance a gamma ray travels in the absorber before interacting and is given by formula(Dogra et al., 2017)

$$MFP = \frac{1}{\mu}\,. \qquad (6)$$

where μ is the linear attenuation coefficient.

III. THEORETICAL AND EXPERIMENTAL MASS ATTENUATION COEFFICIENT STUDIES

The theoretical mass attenuation coefficients values were calculated for photon energy of 662 keV using the NIST XCOM software. The calculated mass attenuation coefficients were compared with those of barite concrete and different materials at the same photon energy(K. J. Singh et al., 2008a). Figure 1 illustrates the comparative results of mass attenuation coefficients with barite concrete and other materials at photon energies of 662 keV. It has been noted that the mass attenuation coefficient values for the prepared samples surpass those of barite concrete and different materials at the photon energies of 662 keV shown in Table 2. Thus, it can be inferred that adding bismuth oxide, lead oxide and tellurium oxide to the glass composition enhances gamma-ray shielding effectiveness. The mass attenuation coefficient increases at gamma-ray energy of 662keV from S1 to S6 with decrease in tellurium oxide and increase of phosphorous pentoxide.The addition of P_2O_5 along with high wt% of Bi_2O_3 increases glass density and electron density, leading to more gamma-ray interactions. This is due to dominance of Compton scattering at this energy (662 keV).The half-value layer (HVL) parameters are determined at photon energies of 662 keV using expression (3), and these values are compared to those of barite concrete. The HVL values of the synthesized samples demonstrate a decreasing trend as the TeO_2 content decreases and are also lower than those of barite concrete and some different types of concretes at photon energy of 662 keV. A smaller HVL value indicates that the material is more effective for radiation shielding in terms of thickness requirements.

Mean free path is calculated using (6) and follows a decreasing order with decrease in MnOas shown in Table 1. Low values of mean free path are the indication of the increase of probability of gamma rays to get attenuate.

IV. RESULTS AND DISCUSSION

Structural analysis of prepared heavy-metal oxide phosphate glasses modified with (MnO) as glass network modifier with stoichiometric composition as 40 Bi_2O_3–35 H_3BO_3–(25−*x*) P_2O_5–*x*MnO**,** where *x* = 0.5, 1.0, 1.5, 2.0 and 2.5 mol% has been performed by studying X-ray diffraction (XRD) patterns. Figure 1 shows x-ray diffraction data of the prepared heavy-metal oxide phosphate glasses modified with (MnO) as glass network modifier. Figure 1 clearly shows broad diffuse halo without any sharpness or well defined bragg's diffraction peak confirms predominantly amorphous nature of prepared heavy-metal oxide phosphate glasses modified with (Mn_2O_3) as glass network modifier.

ISSN: 2321-9653; IC Value: 45.98; SJ Impact Factor: 7.538
Volume 14 Issue VIII Aug 2026- Available at www.ijraset.com

Absence of crystalline in bragg's diffraction peaks indicates that incorporation of metal oxides as mentioned in stoichiometric proportion are incorporated into a disordered glassy matrix and that no detectable long-range structural ordering occurs within the investigated composition range. Broad diffraction peaks as scattering band observed in 2θ ~ 20–40° approximatelymust be attributed to the short-range structural correlations associated with Bi_2-O_3 polyhedral, borate groups and other structural units represent glass network. Position of such broad diffuse halo diffraction peak changes as stoichiometric proportion of (MnO) as glass network increases suggests enhancement in short range connectivity as well as structural arrangement of modified glass network. Amorphous nature of prepared glass network results from absence of diffraction peaks of oxides mentioned in stoichiometric proportion incorporated in disordered glassy matrixdemonstratedthepartial substitution of P_2O_5 with stoichiometric proportion of MnO preserves amorphous structure of heavy-metal oxide phosphate glasses modified with (MnO) as glass network modifier of Bi_2O_3–B_2O_3–P_2O_5-based glass system**,** while producing subtle modifications in its short-range structural arrangement.

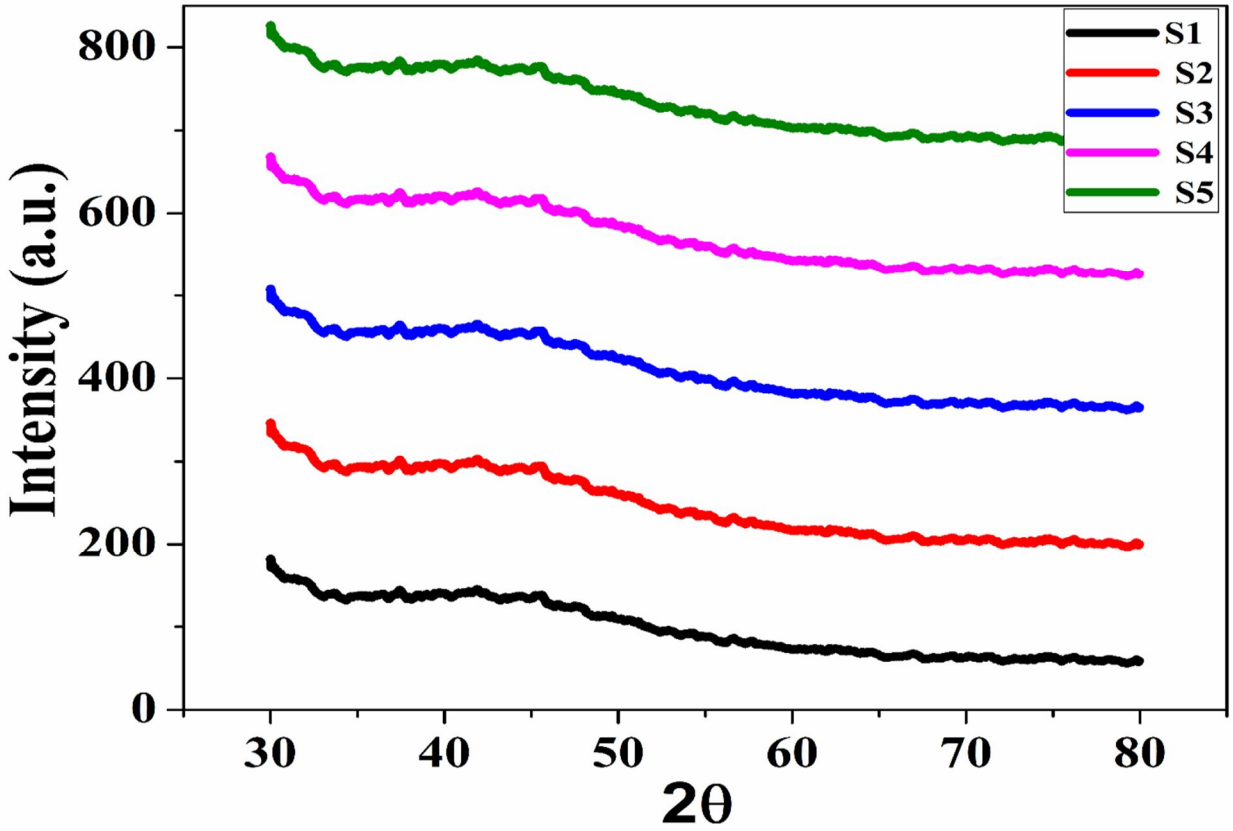

Figure 1: X-ray Diffraction pattern of heavy-metal oxide phosphate glasses modified with (MnO) as glass network modifier

Surface morphological analysis of synthesized heavy-metal oxide phosphate glasses modified with Mn_2O_3 as glass network modifier with stoichiometric proportion of 40 Bi_2O_3–35 H_3BO_3–(25−*x*) P_2O_5–*x*MnO, where *x* = 0.5, 1.0, 1.5, 2.0 and 2.5 mol% has been carried out using SEM micrographs. Figure 2 show micrographs of prepared heavy-metal oxide phosphate glasses modified with MnO as glass network modifier recorded using scanning electron microscopy. SEM image reveals homogeneous relatively smooth and compact surface morphology without irregular crystalline grains arrangement, boundaries or separately arranged regions. The absent of distinct crystallite of constituents according to stoichiometric proportion (Bi_2O_3, H_3BO_2, P_2O_5 and MnO) represents uniform distribution in glass network corresponds to amorphous behavior in consistent with X-ray diffraction data. Subtle variation in morphological signature with increase of substituent (MnO)according to stoichiometric proportion results due to change associated with locally arranged structural network of glass and bonds of phosphate–borate network. Such modification using glass network modifier (MnO) also renew connective network of glass due to Mn-O bonds and also modify concentration of bridging and non-bridging oxygen atoms. In Figure 2, presence of small with multiple shaped feature stamped for stoichiometric variation or changed coordination number. The absence of pores, aggregation or cracks shows successful incorporation of glass modifier (MnO) with good homogeneous distribution.

©IJRASET: All Rights are Reserved | SJ Impact Factor 7.538 | ISRA Journal Impact Factor 7.894 |

ISSN: 2321-9653; IC Value: 45.98; SJ Impact Factor: 7.538
Volume 14 Issue VIII Aug 2026- Available at www.ijraset.com

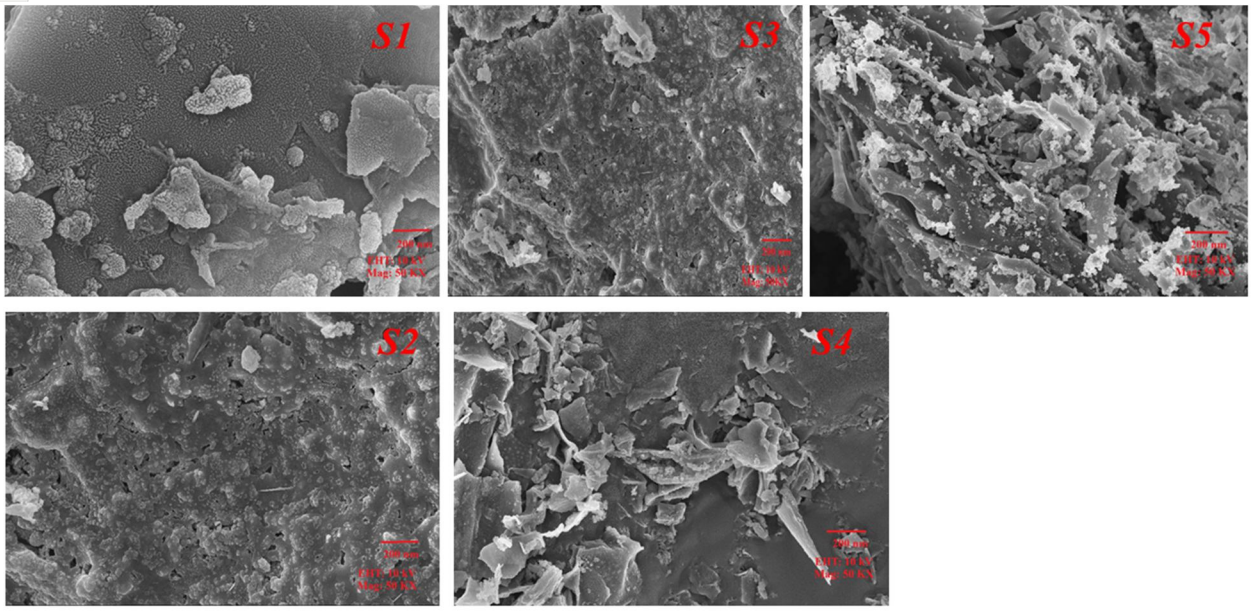

Figure 2: SEM Micrographs of heavy-metal oxide phosphate glasses modified with (MnO) as glass network modifier

Photon radiation attenuation ability of heavy-metal oxide phosphate glasses modified with Mn_2O_3 as glass network modifier with stoichiometric proportion of 40 Bi_2O_3–35 H_3BO_3–(25−*x*) P_2O_5–*x*MnO, where *x* = 0.5, 1.0, 1.5, 2.0 and 2.5 mol% has been intensified and analyzed from Mass Attenuation Coefficient (μ_m) commonly known as *MAC* and Linear Attenuation Coefficient (μ), calculated formulae mentioned in experimental section. The attenuation of prepared heavy metal oxide modified with glass modifier (MnO) has been investigated from slender beam transmitted recorded selected radio isotope (Cs-137-662 keV, Co-60-1173 keV& Co-60-1332 keV) using method known as sum of weighted elemental mass attenuation termed as Mixture rule using relation

$$\mu = \mu_m \cdot \rho$$

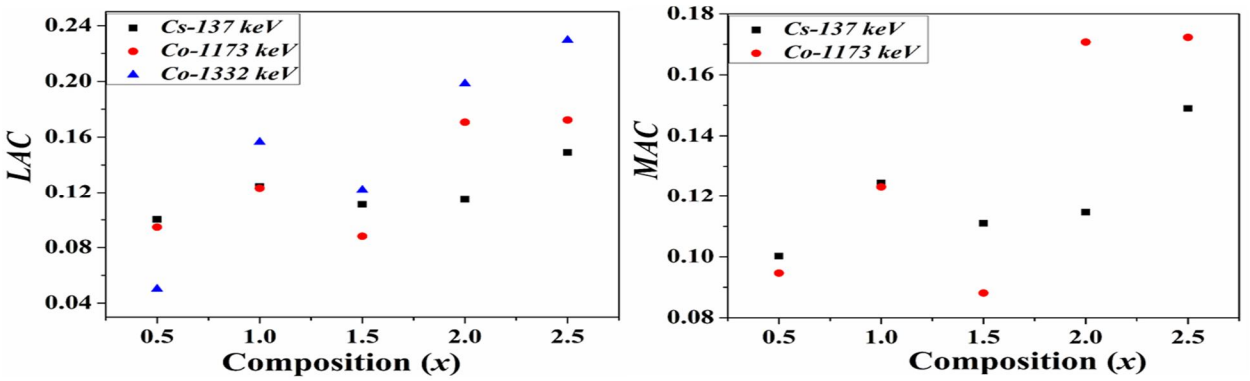

Figure 3: SEM Micrographs of heavy-metal oxide phosphate glasses modified with (MnO) as glass network modifier

Figure 3 shows variation of Linear Attenuation Coefficient & Mass attenuation coefficient vs. Composition (*x*). Figure clearly display significant increase in Linear Attenuation Coefficient & Mass attenuation coefficient with stoichiometric increase of MnOfrom 0.5 to 2.5 mol% at P_2O_5 at pronounced lowest energies. This tailored reflects comprises two coupled effects of partial substitution Manganese (*Z* = 25) from MnO with Phosphorus (*Z* = 15) from P_2O_5arises from effective atomic number of stoichiometric constituents mentioned in stoichiometric composition of heavy-metal oxide phosphate glasses modified with (MnO) as glass network modifierglass which results in strengthening radiation absorption and secondly, partial substitution of MnO with P_2O_5 reticulates glass network of heavy-metal oxide phosphate glasses though crosslinking of P-O-Mn covalent bonds which enhances structural integrity as well as compactness in form of density. As we know

$$\mu \propto \rho$$

©IJRASET: All Rights are Reserved

Therefore, it directly means that glass sample having maximum density exhibit maximum mass as well as linear attenuation as shown in Figure 3.

This enhancement has also been directly evident from increase in mass –density along with Z_{eff}. Role of MnO in densification of glass network has also be identified from estabilished glass network of phosphate matrices which tailored with stoichiometric increment of MnO as mentioned in experimental section. The maximum stoichiometric substitution of MnO enhances radiation (γ radiation) shielding efficiency of ternary heavy-metal oxide phosphate glasses modified with (MnO) as glass network modifierphosphate glasses. The maximum stoichiometric substitution of MnO as glass modifier also impacted HVL & TVL.

Radiation-shielding attenuation response of prepared heavy-metal oxide phosphate glasses modified with MnO glass network modifier with stoichiometric proportion of 40 Bi_2O_3–35 H_3BO_3–(25−*x*) P_2O_5–*x*MnO, where *x* = 0.5, 1.0, 1.5, 2.0 and 2.5 mol%, has been investigated from Half-Value Layer (HVL) which corresponds to 50% attenuation and Tenth-Value Layer (TVL)corresponds to 10%, attenuation of radiation. Figure 4 shows Half-Value Layer (HVL)& Tenth-Value Layer (TVL) vs. Composition (*x*).

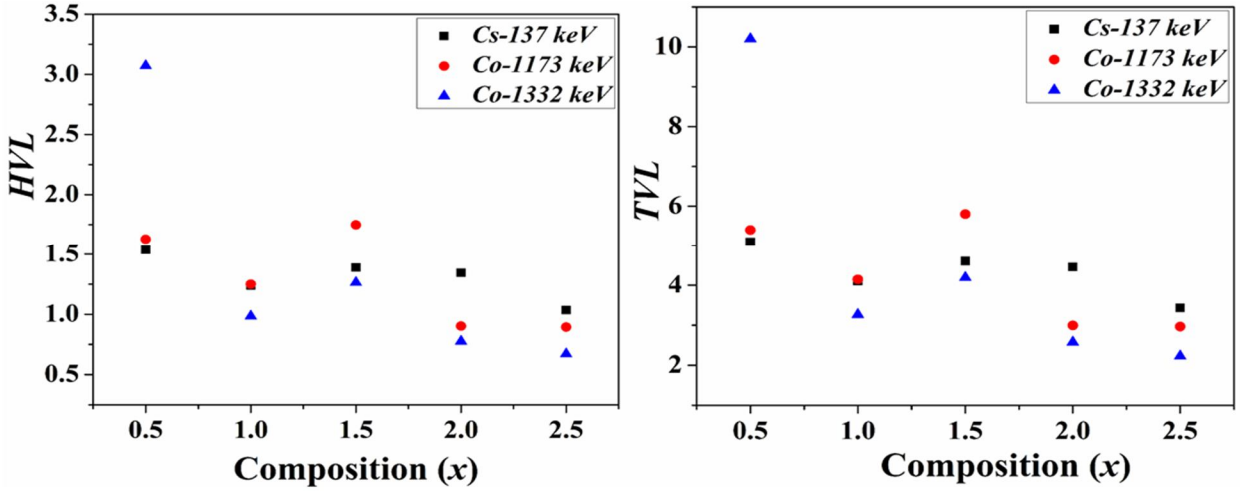

Figure 4: SEM Micrographs of heavy-metal oxide phosphate glasses modified with (MnO) as glass network modifier

The investigation of HVL and TVL have been evaluated for ^{13}Cs (662 keV), 60Co (1173 keV), and 60Co (1332 keV) photon energies. As we know, low value of HVL and TVL indicate towards smaller thickness of prepared heavy-metal oxide phosphate glasses modified with (MnO) as glass network modifier for shielding of γ radiation to 50% & 10% of its original incident radiation intensity. It has been clearly visualizing from Figure 4 that for radio isotope (137Cs), value of HVL decreases from ~1.54 cm at *x* = 0.5 to ~1.23 cm at *x* = 1.0 reveals an increase from ~1.39 cm at *x* = 1.5 and then immediately starts decreasing to ~1.35 & 1.03 cmwhereas for *x* = 2.0 & 2.5 mol%, respectively, it shows non-monotonic behavior. For radio isotope 60Co (1173 keV), value of HVL decreases from ~1.62 cm for *x* = 0.5 to 1.25 cm for *x* = 1.0 results for an increase from ~1.75 cm for*x* = 1.5 then suddenly decreases remarked towards ~0.90 & 0.88 cm at *x* = 2.0 & 2.5 mol%, respectively. For radio isotope 60Co having 1332 keV, value of HVL decreases from ~3.08 cm at *x* = 0.5 to 1.00 cm at *x* = 1.0 reveals increment to ~1.27 cm at *x* = 1.5 and followed by reduction to ~0.78 and 0.68 cm for *x* = 2.0 & 2.5 mol%, respectively. The TVL values also varies in accordance with HVL because of value of has been calculated using formula TVL = 2.303/μ, whereas HVL = 0.693/μ. So both parameters are inversely proportional to the linear attenuation coefficient. The minimum value of TVL calculated to be at 2.5 mol% of stoichiometric proportion of substituent MnOas glass network modifier achieves ~3.4 cm, 2.9 cm and 2.3 cm for 137Cs, 60Co (1173 keV) and 60Co (1332 keV), respectively. Such lowering response of HVL &TVL at higher stoichiometric composition of MnO as glass network modifier for *x* = 2.0 and 2.5 mol%, are in consistent with tailored linear attenuation coefficient response for mentioned stoichiometric compositions.

Mean Free Path (MFP)of heavy-metal oxide phosphate glasses modified with (MnO) as glass network modifier with stoichiometric proportion of 40 Bi_2O_3–35 H_3BO_3–(25−*x*) P_2O_5–*x*MnO, where *x* = 0.5, 1.0, 1.5, 2.0 and 2.5 mol%, has been show in Figure 5. The Mean Free Path (MFP)of heavy-metal oxide phosphate glasses modified with (MnO) as glass network modifierhas been investigated using radio isotopes 137Cs (662 keV), 60Co (1173 keV) & 60Co (1332 keV) photon energies. MFP shows minimum distance travelled by photon radiation shielding heavy-metal oxide phosphate glasses modified with (MnO) before its undergo an interaction according to Linear Attenuation Coefficient as

$$MFP = 1/\mu$$

ISSN: 2321-9653; IC Value: 45.98; SJ Impact Factor: 7.538
Volume 14 Issue VIII Aug 2026- Available at www.ijraset.com

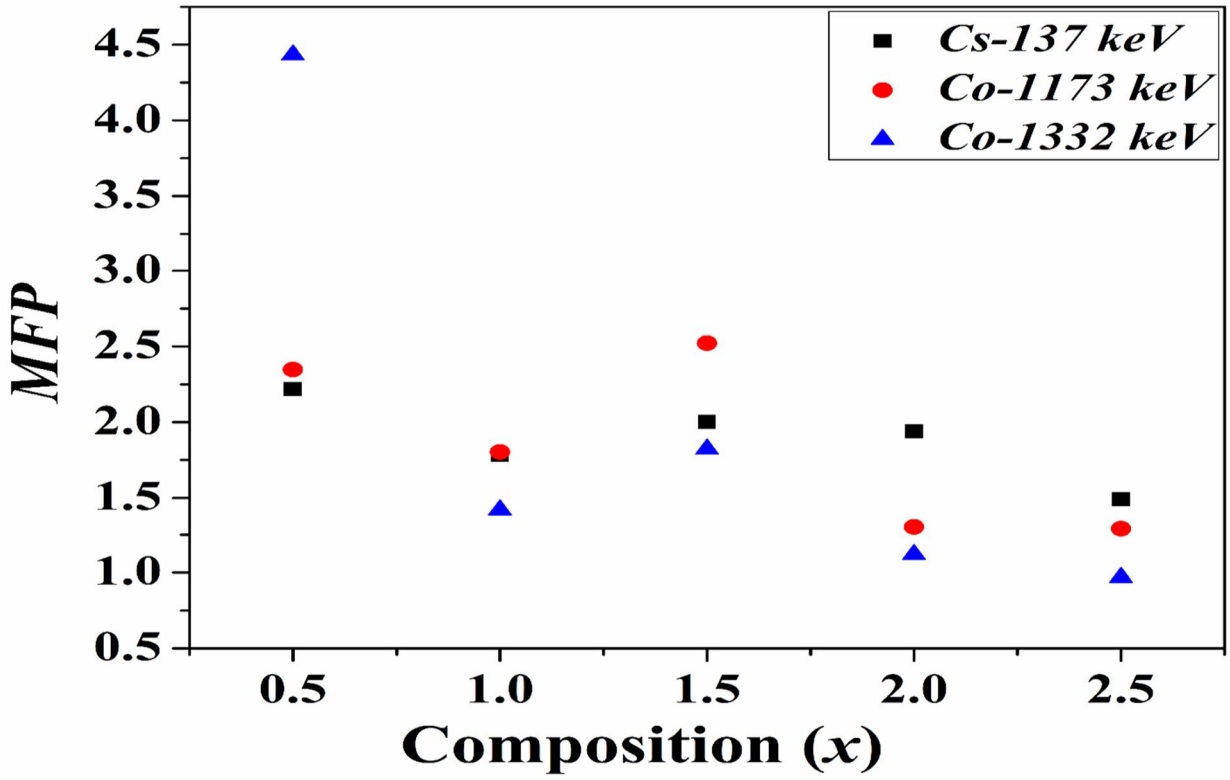

Figure 5: SEM Micrographs of heavy-metal oxide phosphate glasses modified with (MnO) as glass network modifier

It has been clearly visualized from Figure 5 that lower value of MFP stamped for maximum probability of interaction of photon with improved shielding response. As seen in Figure 5 that MFP shows stoichiometric dependence also which stamped from decreasing response as stoichiometric substitution of MnO as glass network modifier increases. For radio isotope 137Cs having energy 662 keV, MFP decreases from ~2.22 cm at x = 0.5 to ~1.78 cm at x = 1.0, followed by an increase from ~2.01 cm at x = 1.5 and then subsequently decreases to ~1.94 and 1.50 cm at x = 2.0 and 2.5 mol%, Almost similar response observed for radio isotope 60Co having energy 1173 keV, where MFP decreases from ~2.35 cm at x = 0.5 to ~1.81 cm at x = 1.0 and then increases to ~2.52 cm at x = 1.5 and again decreases significantly to ~1.31 and 1.30 cm for x = 2.0 &2.5 mol%. For radio isotope 60Co having energy 1332-keV photons, Mean Free Path decreases from ~4.45 cm at x = 0.5 to 1.44 cm at x = 1.0 and then slight increase from ~1.83 cm at x = 1.5, and then starts decreases to ~1.13 & 0.99 cm at x = 2.0 and 2.5 mol%. The smallest value of Mean Free Path for stoichiometric proportion2.5 mol% of glass network modifier (MnO) evident for maximum interaction of photonamong the investigated compositions. The observed response of MFP higher stoichiometric proportion of glass network modifier (MnO) enhances attenuation coefficient to maximum value in association with density of prepared heavy-metal oxide phosphate glasses modified with (MnO) as glass network modifier [11-21].

.Room temperature dielectric permittivity varying with Frequency of heavy-metal oxide phosphate glasses with stoichiometric composition 40 Bi_2O_3–35 H_3BO_3–(25−x) P_2O_5–xMnO, where x = 0.5, 1.0, 1.5, 2.0 and 2.5 mol%, was investigated using Impedance analyzer to cupped effect of MnO incorporation in glass network on polarization mechanism and charge transport behavior shown in Figure 6. Room temperature dielectric permittivity (ε' & ε") vs. Frequency shown in Figure. The dielectric permittivity (ε' & ε") exhibits a pronounced dependence on frequency, exhibits relatively high values in low-frequency region and follows a gradual decrease as frequency increases towardshigh regime. Frequency dependent dielectric permittivity (ε' & ε") eventually approaching an almost frequency-independent region after a particular after approaching a particular value in higher frequency region. The enhanced dielectric permittivity (ε' & ε") in region low frequencies can be signatures of combined contribution of space-charge polarization, interfacial polarization and electrode polarization, which become significant when the applied electric field changes slowly and mobile charge carriers have sufficient time to accumulate at interfaces and electrode–glass boundaries. The direct influence of increasing frequency results in delay in response of charge carriers to follow rapidly alternating frequency of ac signal electric field applied externally.

©IJRASET: All Rights are Reserved | SJ Impact Factor 7.538 | ISRA Journal Impact Factor 7.894 |

ISSN: 2321-9653; IC Value: 45.98; SJ Impact Factor: 7.538
Volume 14 Issue VIII Aug 2026- Available at www.ijraset.com

Due to this, elimination in contribution in some dielectric polarization and hence a decrease in permittivity appears. The incorporation of MnO/Mn-related species as a glass modifier further modifies dielectric response of prepared heavy-metal oxide phosphate glasses by establishing of localized electronic states additionally and formation ofmixed-valence hopping between Mn^{2+}/Mn^{3+} ions which contribute their effect to localized charge transport and polarization. As the MnO as glass network modifier increases according to stoichiometric proportion increases from 0.5 to 2.5 mol%, value of dielectric permittivity (ε' & ε")changes directly signature continuoustailoring in network ofheavy-metal oxide phosphate glasses modified with (MnO) as glass network modifier. Such change in stoichiometric substitution of MnO as glass network modifier also responsibleenhancement in the formation of concentration of non-bridging oxygen ions according to stoichiometric proportion of glass network modifier avails localized charge carriers. At higher frequencies, dielectric permittivity (ε' & ε")decrease due mismatch in response of r polarization mainly electronic and ionic polarizationwith externally applied electric field which reorientnumber of dipoles in according to externally applied electric field. Due to such fast orientation of externally applied electric, some polarization due to inertia of dipoles not matches at considerably at high frequency. So overallobservedfrequency dispersion response confirms typical dielectric behavior in amorphous heavy-metal oxide phosphate glasses with stoichiometric composition 40 Bi_2O_3–35 H_3BO_3–(25−*x*) P_2O_5–*x*MnO, where *x* = 0.5, 1.0, 1.5, 2.0 and 2.5 mol%, demonstrates that MnO incorporation provides an effective means of tailoring their dielectric properties for potential electronic, dielectric and ionic conducting applications [22-26].

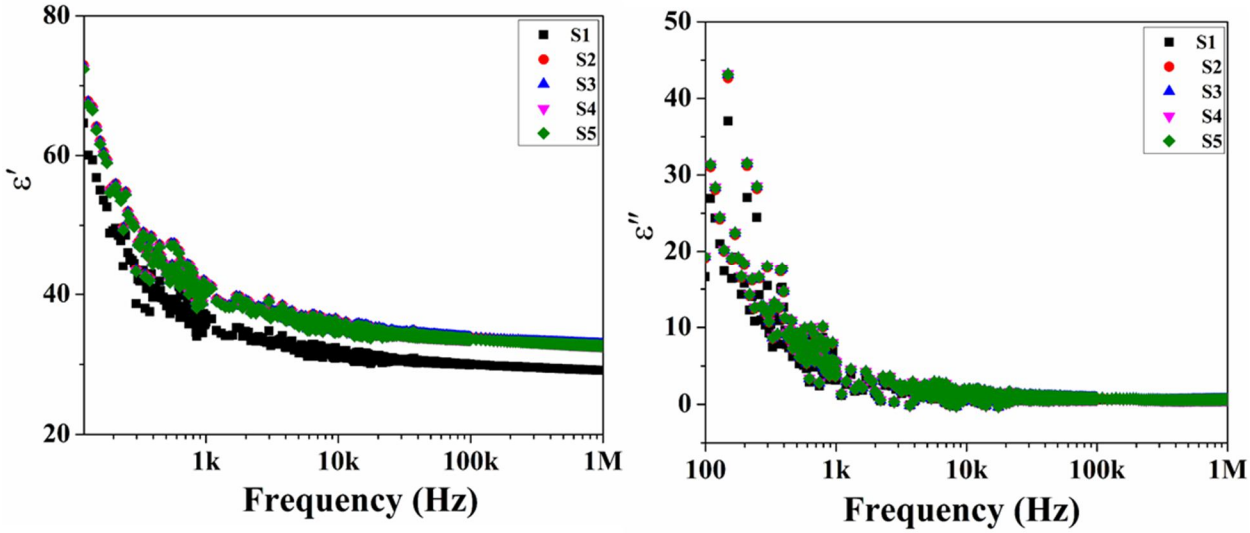

Figure 6: Dielectric permittivity (ε' & ε")vs. Frequency (Hz) of heavy-metal oxide phosphate glasses modified with (MnO) as glass network modifier

Room temperature Frequency-dependent electrical conductivity of the prepared heavy-metal oxide phosphate glasses with stoichiometric proportion of 40 Bi_2O_3–35 H_3BO_3–(25−*x*) P_2O_5–*x*MnO, where *x* = **0.5, 1.0, 1.5, 2.0 and 2.5 mol%**, have been investigated for electric conduction. Room temperature σ_{ac} vs. Frequency (Hz) investigated at room temperature has been shown in Figure 7. It has been clear visualized from conductivity spectra that is MnO increases, a characteristic increase in electrical conductivity with increasing frequency for heavy-metal oxide phosphate glasses modified with MnO glass modifier appears. Integration of MnO into these heavy-metal oxide networks serves to further stabilize the glass matrix network which induces structural compaction and facilitates significant changes by establishing an intricate relationship between structural defects and the hopping of charge carriers. The conductivity profile has been bifurcated in region. First is frequency independent region commonly termed as dc conductivity (σ_{dc}) whereas frequency dependent region named as ac conductivity (σ_{ac}). The conductivity profile has been analyzed by **Jonscher universal power law**,

$$\sigma(\omega)=\sigma_{dc}+A\omega^{s},$$

Where σ_{dc}represents the frequency-independent conductivity, A is a temperature-dependent constant, ω is the angular frequency, and s is the frequency exponent [26-27].

©IJRASET: All Rights are Reserved | SJ Impact Factor 7.538 | ISRA Journal Impact Factor 7.894 |

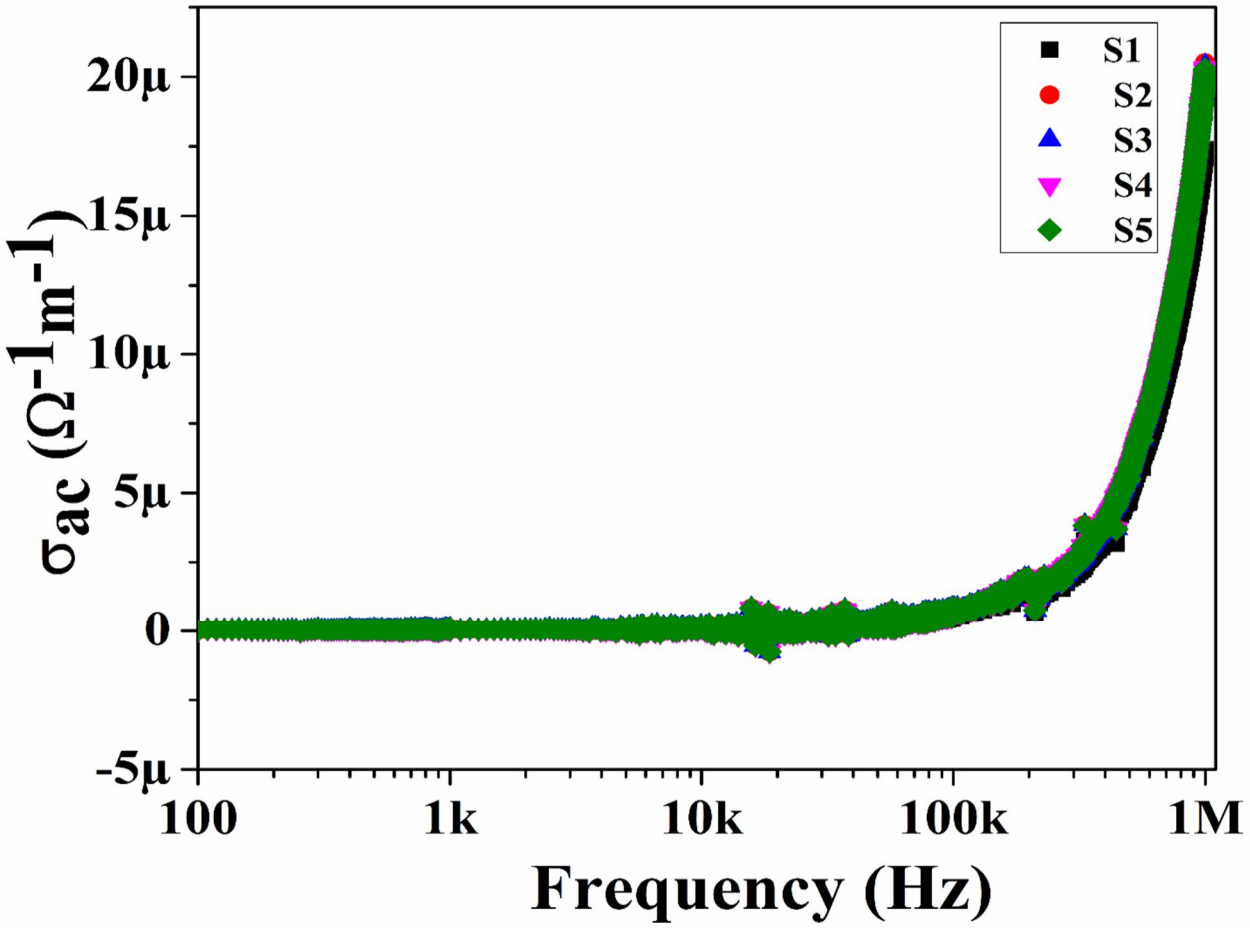

Figure 7: Dielectric permittivity (ε' & ε")vs. Frequency (Hz) of heavy-metal oxide phosphate glasses modified with (MnO) as glass network modifier

It has been clear visualized from Figure 7 that Stoichiometric incorporation of manganese ions from MnO in matrix of heavy-metal oxide phosphate glasses tailor electronic transport ability results in non-debye relaxation response which provides information of activation energy distribution due to charge carriers dynamics. Incorporation of MnO in matrix of Glass responsible for tailoring conductivity due to multivalent Mn (Mn^{3+}/Mn^{2+}) which results in small polaron hopping and electronic transport behavior. The stoichiometric variation of MnO within heavy-metal oxide phosphate glasses Bi-Borate phosphate glasses forms potential barriers which dictate dielectric relaxation. The small polaron hopping results due to occupation of octahedral site which responsible for electron transfer formed hopping of Mn into of $Mn^{3+}$and Mn^{2+}.

V. CONCLUSION

This research explores the impact of MnO doping on the structural and gamma-ray shielding characteristics of bismuth borate glasses. Important key properties such as mass attenuation coefficient (MAC), half-value layer (HVL), density, optical behavior, and elastic parameters were calculated. Experimental MAC values, measured using using radio isotopes 137Cs (662 keV), 60Co (1173 keV) & 60Co (1332 keV) photon energies. We observe that systematic growth of both attenuation coefficients with MnO content confirms that manganese acts as an effective modifier that enhances the gamma-ray shielding competence of the bismuth boro-phosphate glasses studied here. The results also confirm that controlled MnO incorporation can effectively tailor the radiation attenuation characteristics of Bi_2O_3-rich phosphate glasses, making them promising candidates for compact gamma-radiation shielding applications.MFP results corroborate the HVL, TVL, MAC and LAC findings and confirm that the $40Bi_2O_3$–$35H_3BO_5$–$22.5P_2O_5$–2.5MnO glass exhibits the most favorable photon-shielding characteristics among the studied compositions, making it a promising candidate for gamma-radiation shielding applications.

REFERENCES

[1] A.Al-Yousef, H., Alotiby, M., Kumar, A., Alotaibi, B. M., Alsaif, N. A. M., Sayyed, M. I., Mahmoud, K. A., & Al-Hadeethi, Y. (2021). Physical, structural, and gamma ray shielding studies on novel (35+x) PbO-5TeO_2-20Bi_2O_3-(20-x) MgO-20B_2O_3 glasses. Journal of the Australian Ceramic Society, 57(3), 971–981. https://doi.org/10.1007/s41779-021-00600-6

[2] Abdel-Baki, M., Abdel-Wahab, F. A., Radi, A., & El-Diasty, F. (2007). Factors affecting optical dispersion in borate glass systems. Journal of Physics and Chemistry of Solids, 68(8), 1457–1470. https://doi.org/10.1016/j.jpcs.2007.03.026

[3] Abdelghany, A. M., ElBatal, H. A., &Marei, L. K. (2012). Optical and shielding behavior studies of vanadium-doped lead borate glasses. Radiation Effects and Defects in Solids, 167(1), 49–58. https://doi.org/10.1080/10420150.2011.629418

[4] Callister, W. D. (2019). Materials Science and Engineering. Wiley.

[5] Damodaran, K. V., & Rao, K. J. (1989). Elastic properties of phosphotungstate glasses. Journal of Materials Science, 24(7), 2380–2386. https://doi.org/10.1007/BF01174499

[6] Dogra, M., Singh, K. J., Kaur, K., Anand, V., & Kaur, P. (2017). Gamma ray shielding and structural properties of PbO-P_2O_5-Na_2WO_4 glass system. 070019. https://doi.org/10.1063/1.4980454

[7] Elsafi, M., Sayyed, M. I., Hanafy, T. A., More, C. V., &Hedaya, A. (2024). Experimental study of gamma-ray attenuation capability of B_2O_3-ZnO-Na2O-Fe_2O_3 glass system. Scientific Reports, 14(1), 19141. https://doi.org/10.1038/s41598-024-68941-3

[8] Kaur, K., Singh, K. J., &Anand, V. (2015). Correlation of gamma ray shielding and structural properties of PbO–BaO–P_2O_5 glass system. Nuclear Engineering and Design, 285, 31–38. https://doi.org/10.1016/j.nucengdes.2014.12.033

[9] Kaur, K., Singh, K. J., &Anand, V. (2016). Structural properties of Bi_2O_3–B_2O_3–SiO_2–Na_2O glasses for gamma ray shielding applications. Radiation Physics and Chemistry, 120, 63–72. https://doi.org/10.1016/j.radphyschem.2015.12.003

[10] Kolavekar, S. B., Hiremath, G. B., Patil, P. N., Badiger, N. M., &Ayachit, N. H. (2022). Investigation of gamma-ray shielding parameters of bismuth phospho-tellurite glasses doped with varying Sm_2O_3. Heliyon, 8(11), e11788. https://doi.org/10.1016/j.heliyon.2022.e11788

[11] Kumar, A. (2017). Gamma ray shielding properties of PbO-Li 2 O-B_2O_3 glasses. Radiation Physics and Chemistry, 136, 50–53. https://doi.org/10.1016/j.radphyschem.2017.03.023

[12] Maeder*, T. (2013). Review of Bi_2O_3 based glasses for electronics and related applications. International Materials Reviews, 58(1), 3–40. https://doi.org/10.1179/1743280412Y.0000000010

[13] Peterson, R. S. (1996). Experimental γ ray spectroscopy and investigations of environmental radioactivity. Spectrum Techniques, 6. https://physicsx.erau.edu/Courses/CoursesS2023/PS315/NuclearSpectroscopy/Nuclear%20Spectroscopy.pdf

[14] Singh, K. J., Singh, N., Kaundal, R. S., & Singh, K. (2008a). Gamma-ray shielding and structural properties of PbO–SiO_2 glasses. Nuclear Instruments and Methods in Physics Research Section B: Beam Interactions with Materials and Atoms, 266(6), 944–948. https://doi.org/10.1016/j.nimb.2008.02.004

[15] Singh, K. J., Singh, N., Kaundal, R. S., & Singh, K. (2008b). Gamma-ray shielding and structural properties of PbO–SiO_2 glasses. Nuclear Instruments and Methods in Physics Research Section B: Beam Interactions with Materials and Atoms, 266(6), 944–948. https://doi.org/10.1016/j.nimb.2008.02.004

[16] Singh, K., Singh, H., Sharma, V., Nathuram, R., Khanna, A., Kumar, R., Singh Bhatti, S., & Singh Sahota, H. (2002). Gamma-ray attenuation coefficients in bismuth borate glasses. Nuclear Instruments and Methods in Physics Research Section B: Beam Interactions with Materials and Atoms, 194(1), 1–6. https://doi.org/10.1016/S0168-583X(02)00498-6

[17] Singh, N., Singh, K. J., Singh, K., & Singh, H. (2004). Comparative study of lead borate and bismuth lead borate glass systems as gamma-radiation shielding materials. Nuclear Instruments and Methods in Physics Research Section B: Beam Interactions with Materials and Atoms, 225(3), 305–309. https://doi.org/10.1016/j.nimb.2004.05.016

[18] Urbach, F. (1953). The Long-Wavelength Edge of Photographic Sensitivity and of the Electronic Absorption of Solids. Physical Review, 92(5), 1324–1324. https://doi.org/10.1103/PhysRev.92.1324

[19] Wongsing, T., Kaewkhao, J., Limsuwan, P., &Kedkaew, C. (2012). Formation and Optical Absorption of CuO-Doped SLS System. Procedia Engineering, 32, 807–813. https://doi.org/10.1016/j.proeng.2012.02.016

[20] Yamane, M., & Mackenzie, J. D. (1974). Vicker's Hardness of glass. Journal of Non-Crystalline Solids, 15(2), 153–164. https://doi.org/10.1016/0022-3093(74)90044-1

[21] Yin, S., Wang, H., Li, A., Ma, Z., & He, Y. (2022). Study on Radiation Shielding Properties of New Barium-Doped Zinc Tellurite Glass. Materials (Basel, Switzerland), 15(6), 2117. https://doi.org/10.3390/ma15062117

[22] KumarM, YadavKL. J. Phys.: Condens. Matter. 2002; 19:242202.

[23] ColeKS, RobertH. Dispersion and Absorption in Dielectrics:- Alternating Current Characteristics. Journal of Chemical Physics. 1941; 9:341–351.

[24] HavriliakS, NegamiS. A complex plane representation of dielectric and mechanical relaxation processes in some polymers. Polymer. 1967;8:161-210. DOI: 10.1016/0032-3861 (1967) 90021-3.

[25] JonscherAK. The Universal dielectric response. Nature. 1977; 267:673-679.

[26] Vaish R, VarmaKBR. Dielectric properties of Li_2O-3B_2O_3glasses. J. Appl. Phys. 2009; 103:064106.

[27] Megdiche M, Pellegrino CP, Gargouri M. Conduction mechanism study by overlapping large Polaron tunneling model in $SrNiP_2O_7$ ceramic compound. J Alloys Compd. 2014; 584:209-215.

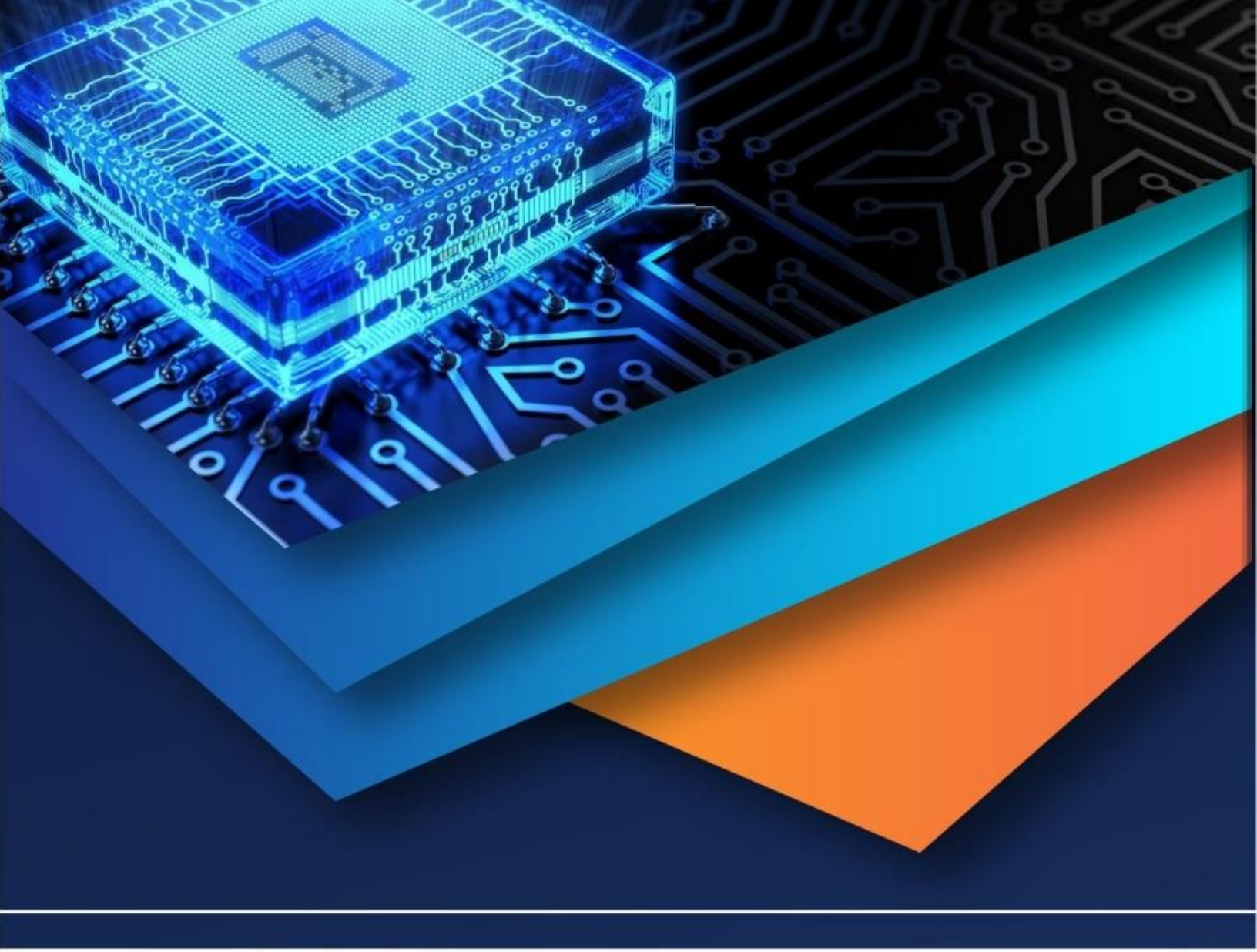

10.22214/IJRASET

45.98

IMPACT FACTOR: 7.129

IMPACT FACTOR: 7.429

INTERNATIONAL JOURNAL FOR RESEARCH

IN APPLIED SCIENCE & ENGINEERING TECHNOLOGY

Call : 08813907089 (24*7 Support on Whatsapp)